




Original Paper

Journal of Innovative Engineering
and Natural Science

(Yenilikçi Mühendislik ve Doğa Bilimleri Dergisi)

<https://dergipark.org.tr/en/pub/jiens>

Seismic vulnerability and risk assessment of a typical RC school building using hybrid-based fragility curves

 Ali Yeşilyurt^{a,*}
^aDepartment of Earthquake Engineering, Disaster Management Institute, Istanbul Technical University, 34469, Istanbul, Türkiye.

ARTICLE INFO

Article history:

Received 18 April 2025

Received in revised form 16 June 2025

Accepted 5 July 2025

Available online

Keywords:

Fragility Curve

Vulnerability Assessment

Seismic Risk

School Building

Capacity Curve

ABSTRACT

Seismic risk assessment is a critical process for quantifying the expected structural damage and economic losses resulting from seismic events. Such studies are essential for developing effective pre-earthquake preparedness strategies and ensuring the efficient implementation of post-earthquake response plans. In this study, the seismic vulnerability and risk assessment of a typical low-rise reinforced concrete school building with shear wall systems, located at various locations in the province of Adıyaman, was carried out. First, a three-dimensional finite element model of the school building was developed. Subsequently, a nonlinear static (pushover) analysis was performed to obtain the capacity curve of the building. Based on three different empirical models, hybrid-based fragility curves were derived as a function of spectral acceleration. Furthermore, vulnerability curves were constructed using twelve different consequence models. A scenario-based seismic hazard analysis was conducted for the Narince segment, one of the active fault lines in the South-eastern Anatolia Thrust. As a result of the risk assessment, considering the proposed vulnerability models, the expected loss ratio values were computed at different locations. When the results are evaluated as a whole, it is observed that the loss values of the building vary significantly depending on the location. While certain locations are expected to experience irreparable damage, others are likely to sustain only minor, repairable damage. This study serves as a significant example for assessing the seismic risk of typical school building types. The proposed methodology and findings, if extended to other similar typologies, can facilitate the development of a comprehensive and regional-scale seismic risk assessment framework for school buildings.

I. INTRODUCTION

Schools should be safe buildings where children and young people receive an education and develop into responsible individuals. Students and teachers spend a considerable amount of time in these spaces. It is, therefore, vital that school buildings not only support educational activities but are also resilient to unforeseen natural disasters. In particular, during events such as earthquakes, the seismic resistance of school buildings is a critical issue in ensuring the safety of students and teachers. Improving the seismic resistance of these structures ensures that, in the event of an earthquake, the buildings will remain standing without collapsing and that people can be evacuated safely. In this context, prioritizing seismic safety measures in the design and construction of school buildings not only strengthens the physical infrastructure but also represents a significant investment in the future of society.

Although the exact timing of an earthquake cannot be predicted, the potential losses it may cause can be estimated in advance. Seismic risk assessment and loss estimation play a crucial role in minimizing earthquake-induced losses and planning post-disaster preparedness. Through such studies, it is possible to identify priority areas for intervention in a specific region following an earthquake. Such studies also help to educate and raise public awareness, facilitate the planning of workforce requirements for disaster management, support budgetary

*Corresponding author. Tel.: +90-507-863-7315; e-mail: aliyesilyurt@itu.edu.tr

allocation processes, and enable the systematic implementation of structural retrofitting measures for existing buildings. The first step in reducing seismic risk, particularly in school infrastructure, is to assess structural performance accurately under potential earthquake scenarios. These assessments are essential for ensuring life safety and maintaining educational continuity, making them a critical component of seismic resilience planning.

Fragility curves are widely used tools for assessing the seismic vulnerability and risk of structures. These are highly practical functions that estimate the probability of exceeding a specified damage state for a given intensity measure value. Therefore, the derivation and implementation of fragility curves represent a common and effective strategy for conducting reliable risk analyses and supporting decision-making processes both before and after earthquakes, particularly within the framework of large-scale risk mitigation actions [1, 2].

Fragility curves can generally be derived using four main approaches: empirical/observational, analytical/numerical simulation-based, hybrid, and expert judgment-based methods [3, 4]. The first of these, empirical methods, is based on fitting assumed statistical models to post-earthquake observational data on damaged buildings [5]. Since they are based on real post-earthquake damage observations, empirical fragility curves are often considered the most reliable. However, limitations such as insufficient post-earthquake damage data in certain regions, inaccuracies in visual damage assessments, and uncertainties in ground motion intensity maps can significantly affect the reliability of the derived curves [6]. In the absence of empirical data, an analytical approach is widely used [7]. This method involves developing numerical models for a specific structure or class of structures, subjecting them to a suite of earthquake ground motions, and conducting structural analyses to statistically evaluate the relationship between intensity measures (IM) and engineering demand parameters (EDP). With advancements in computational capability, ground motion prediction models, and earthquake engineering research, analytically based fragility curves have become increasingly prevalent [8]. This approach also allows for a more detailed consideration of factors such as building configurations, plan irregularities, material properties, and connection details, often underrepresented in empirical models [9]. Nevertheless, analytically derived fragility curves should be validated through observed damage data to ensure their accuracy and reliability. The hybrid approach, as the name suggests, combines both empirical and analytical methods. In this approach, numerical models of target structures are used to derive capacity curves, from which key performance points are identified. These points are then correlated with different damage states using empirical relationships, allowing for the development of hybrid fragility curves. This method can benefit from the strengths of both empirical data and analytical modelling, resulting in a more comprehensive and balanced assessment of seismic vulnerability [10, 11]. Although less frequently utilized in recent years compared to other methods, the limited availability of post-earthquake observational data for various building types in empirical fragility function development, as well as time constraints associated with analytical methods, have necessitated the use of expert judgment-based fragility curves in certain cases. Such expert-based fragility assessments, particularly developed for specific building types, have been documented in studies such as ATC-13 (1985) and ATC-21 (1988) [12, 13].

School buildings typically differ from residential structures in terms of design configurations, construction materials, existing damage from previous earthquakes, age-related degradation, and structural complexity. Features such as irregularities in plan and elevation, variations in material properties and mass distribution, and distinct geometric characteristics, which are especially prominent in school buildings, necessitate treating these structures as a separate building class in fragility assessments. Therefore, in order to improve the accuracy of

seismic risk evaluations and to reduce structural uncertainty, school buildings should not only be analysed independently of residential structures but also be further subcategorized into detailed subclasses based on their specific structural attributes. This stratified approach would allow for the development of more representative and precise fragility curves, ultimately supporting more effective risk mitigation and decision-making strategies [14]. A review of the existing literature reveals that the majority of fragility-related research has focused on residential buildings, while educational buildings, such as schools, have received relatively less attention. Although fragility curves developed for residential structures are sometimes adapted for use with school buildings, this practice may lead to inaccurate risk assessments. This is primarily because general fragility functions, often developed based on simple and common residential typologies, do not adequately account for the unique structural characteristics of school buildings. Domaneschi et al. (2021) have presented a method for real-time seismic vulnerability assessment of existing school buildings using wireless sensor networks [15]. Similarly, an empirical prediction model that allows the direct derivation of fragility curves has been proposed by Gioiella et al. (2023) for predicting seismic damage and expected retrofit costs immediately after earthquakes [16].

The assessment of the seismic vulnerability of existing school buildings in Italy was achieved by O'Reilly et al. (2018), considering sample building typologies (Reinforced concrete frame with masonry infill (RC), Unreinforced masonry (URM), and Precast RC frame (PC)). Fragility curves for the collapse safety damage state were developed as a function of Spectral acceleration (S_a). Subsequently, a case risk estimation study is performed for the defined Expected Annual Loss (EAL) parameter [17]. Following the sequence of earthquakes in Gorkha, empirical fragility curves were developed by Adhikari and Gautam (2019) using data from more than 5,000 damaged RC and masonry school buildings [18]. Samadian et al. (2019) developed fragility and vulnerability curves for a high school building in Tehran, which was constructed in 2000 and then retrofitted with reinforced concrete shear walls. Subsequently, the risk assessment of the target structure in its original and retrofitted state was performed considering the parameters of recovery time and resilience index parameters for different seismic hazard levels [19]. Ruiz-García et al. (2021) have designed the typical 1-3 story representative school building models using the outdated 1990s seismic design code. Drift-based fragility curves were obtained for further comparative analysis. Retrofit recommendations for the existing building class were made with reference to the results obtained in this study [20]. Sathurshan et al. (2023) investigated the seismic vulnerability of lightweight reinforced concrete (RC) school buildings in Sri Lanka. In this study, fragility curves and damage probability matrices are presented for four different damage thresholds using the static nonlinear analysis (push-over) method [21]. The applicability of machine learning (ML) algorithms to enhance rapid screening of schools to establish seismic vulnerability insights with high accuracy and reliability was investigated by Zain et al. 2024 [22].

II. EXPERIMENTAL METHOD / TEORETICAL METHOD

2.1 Seismic Performance of Türkiye School Buildings

Past and recent earthquakes in Türkiye have caused significant structural damage to school buildings, highlighting the urgent need to better understand their potential seismic vulnerabilities [23]. In this context, Oyguc and Guley (2017) conducted an in-depth field investigation of two reinforced concrete school buildings that were damaged during the Mw 7.2 Van Earthquake on October 23, 2011. Numerical models of these buildings were developed, followed by both static and dynamic analyses. Based on the results obtained, several recommendations were

proposed to enhance the seismic resilience of such structures [24]. In a related study, Oyguc (2016) examined the seismic performance of school buildings following the 2011 Van earthquakes. Through on-site investigations, the study identified common types of damage observed in affected schools and emphasized that the key parameters influencing their seismic performance were the quality of construction and the detailing of reinforcement [25]. Similarly, the primary causes of severe damage or collapse in school buildings during the Van Earthquake were thoroughly investigated by Bal and Smyrou (2016). Their findings revealed that various structural deficiencies played a significant role in the vulnerability of these educational facilities to seismic events [26]. Figure 1 shows school buildings that were damaged in the Mw 7.7 and Mw 7.6 Kahramanmaras earthquakes, which were epicentred in Pazarcik and Elbistan, respectively [27].



Figure 1. School buildings that sustained heavy damage during the Kahramanmaras earthquakes [27]

Within the scope of the Istanbul Seismic Risk Mitigation and Emergency Preparedness Project (ISMEP), 856 existing school buildings in Istanbul with insufficient seismic performance have been retrofitted, and 367 school buildings have been reconstructed [28]. Nevertheless, vulnerability assessments conducted for existing school buildings in Türkiye are quite limited. Sediq and Harmandar conducted a seismic vulnerability and risk analysis of a school building located in the Milas district of Mugla. For this purpose, the capacity curve of the existing school building was obtained through static nonlinear analysis. Subsequently, fragility curves were developed using various empirical functions found in the literature [11]. Hancilar et al. (2014) evaluated the vulnerability of typical school buildings located in Istanbul. In this study, considering structural uncertainty, analytical-based fragility curves were presented as a function of the Peak Ground Acceleration (PGA), Peak Ground Velocity (PGV), and Spectral Acceleration (S_a) intensity parameters [29]. Mazılıgüney et al. (2013) developed fragility curves for typical 3, 4, and 5-story school buildings as a function of different intensity parameters [30].

2.2 Scenario-Based Seismic Hazard Analysis for the Narince Segment

Seismic hazard analysis aims to estimate ground motion intensity parameters at a specific location that may be induced by a potentially destructive earthquake. Such analyses are critical for minimizing potential casualties and property damage and for guiding seismic risk mitigation strategies. Adıyaman Province, located in southeastern Türkiye, is situated in a tectonically active region under the influence of the Arabian Plate and the Anatolian Plate. One of the fundamental seismic sources in this region is the Southeastern Anatolian Thrust Zone. This thrust

system extends approximately 1,356.72 km and comprises multiple segments with distinct geometric and kinematic properties, including the Çubuklu, Çüngüş, Gerger, Konalga, Kozluk, Lice, Narince, and Şirvan segments [31]. These fault segments can generate earthquakes of magnitude 6.5 or greater.

Probabilistic Seismic Hazard Analysis (PSHA) and Deterministic Seismic Hazard Analysis (DSHA) are the two main approaches widely used in seismic hazard assessment. In the current study, the DSHA approach is employed. By considering the characteristics of known active faults, the method focuses on assessing the impact of the maximum credible earthquake scenario. Within the scope of this study, the Narince segment- located to the south of the Çelikhan and Gerger districts of Adıyaman Province- was considered. According to the Active Fault Map of Türkiye, this segment exceeds 140 km in length and is known to be capable of producing high-magnitude earthquakes (Figure 2a). Furthermore, the ten locations selected for risk assessment of the school building are indicated in Figure 2a.

Based on the identified segment, a scenario-based seismic hazard analysis was conducted, assuming a moment magnitude (M_w) of 6.9. The analysis was performed using OpenQuake, an open-source seismic hazard and risk modeling platform developed by the Global Earthquake Model (GEM) Foundation [32]. In this assessment, the ground motion prediction equation (GMPE) proposed by Boore et al. (2014) was employed to estimate ground motion intensities [33]. As illustrated in Figure 2b, which displays the distribution of the PGA parameter, the scenario-based hazard analysis indicates that the maximum PGA value for Adıyaman Province reaches up to 0.6 g. Additionally, the distributions of the S_a values at 0.2 seconds [$S_a(0.2s)$] and 1.0 seconds [$S_a(1.0s)$] are presented in Figure 3.

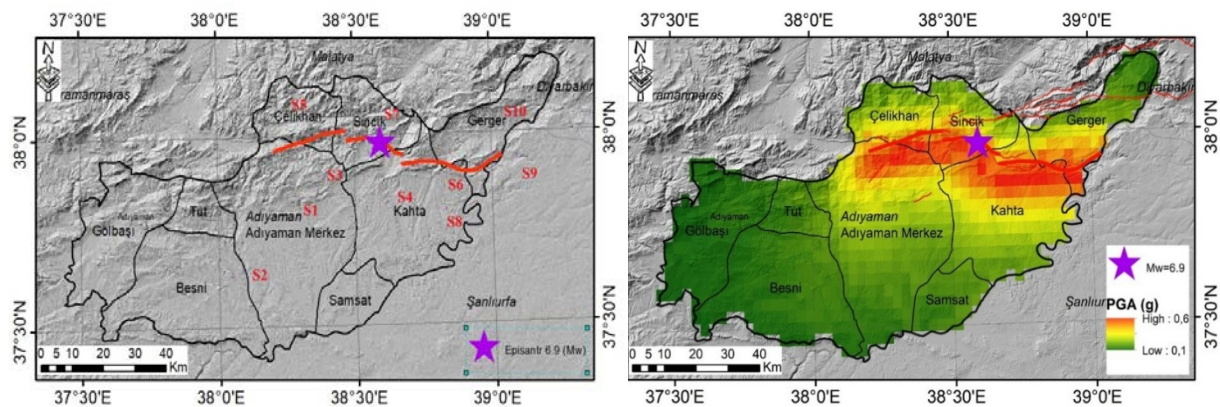


Figure 2. Seismicity of Adıyaman province; a) Location and extent of the Narince segment (left), b) Spatial distribution of PGA values (right)

The response spectra computed for the selected locations under the scenario of a rupture along the Narince segment are presented in Figure 4. Upon examining Figure 4, it is observed that, in the event of a rupture along the Narince segment, the lowest $S_a(T1)$ values corresponding to the calculated period values in both directions of the structure are obtained at location S2, located south of the Adıyaman city center. In contrast, the highest $S_a(T1)$ values are observed at location S6, located in the Narince Bucağı region.

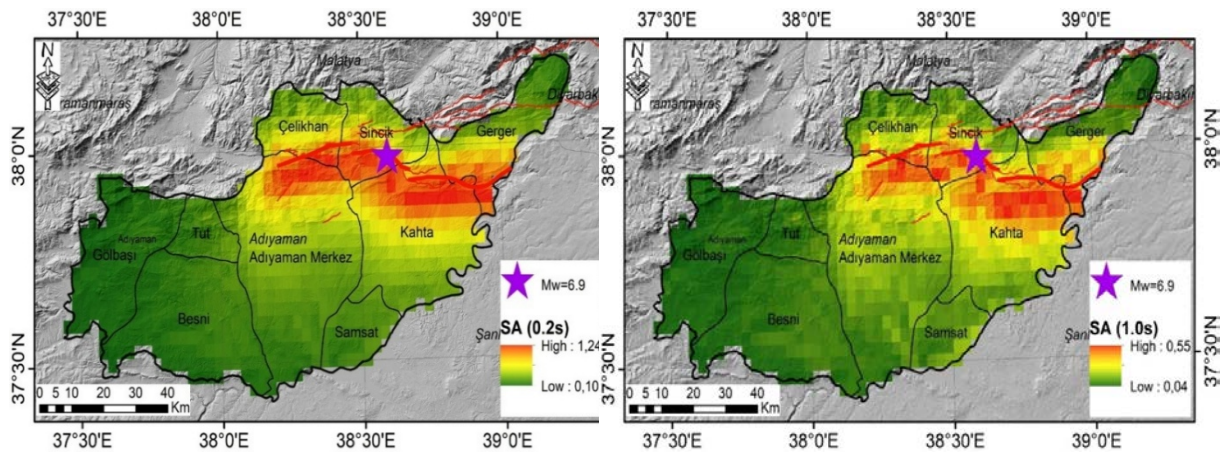


Figure 3. Spectral acceleration distribution across the study area; a) Sa(0.2s) (left), b) Sa(1.0s) (right)

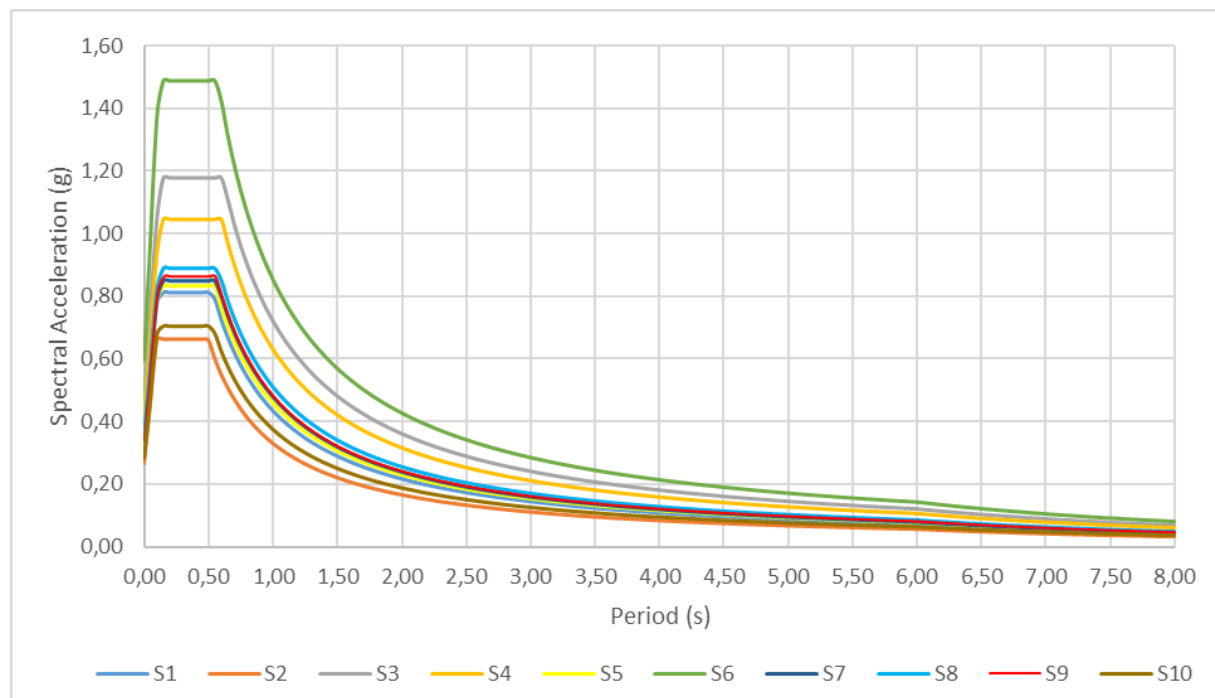


Figure 4. Target spectral curves corresponding to the selected locations

2.3 Vulnerability Analysis of a Typical RC School Building

Fragility curves represent the probability of exceeding a specific damage state (DS) for a given intensity measure (IM) value. These curves are derived by calculating the probability of reaching or exceeding a specified damage state for a given demand measure (DM), as expressed in Equation 1.

$$P_{i,j} = P(DM \geq DS_i | IM_j) \quad (1)$$

For each value of the seismic intensity measure (IM_i), the probability of reaching or exceeding a specific damage state limit (DS_i) for the demand measure (DM) is calculated, as shown in Equation 1. Fragility curves are derived for each damage state using two statistical parameters: the median (IM_{DS_i}) and the standard deviation (β_{DS_i}), as expressed in Equation 2:

$$P[DM \geq DS_i | IM] = \Phi \left(\frac{\ln(IM) - \ln IM_{DS_i}}{\beta_{DS_i}} \right) \quad (2)$$

In Equation (2), Φ represents the cumulative standard log-normal distribution function. In this study, a typical school building located in Adıyaman, which was constructed based on the TEC-2007, is considered. This structure corresponds to the "low-rise reinforced concrete frame with shear wall (C2L), moderate code RC buildings" category in the classification provided in the FEMA 2010 guidelines. The seismic vulnerability and risk assessment of the building will be performed through fragility curves obtained via a hybrid method. In this context, a 3D finite element model of the target structure was initially created. Subsequently, a capacity curve was obtained using the static nonlinear analysis method. Fragility curves were then derived by applying commonly used empirical functions to specific points defined on the obtained capacity curve. In the final section of the study, scenario-based seismic hazard analysis results for the Narince segment, detailed in Section 3, are used along with the derived vulnerability curves to calculate the Expected Loss Ratio (ELR) values.

2.4 Nonlinear Static Analysis (Push-Over)

A typical high school building, consisting of one basement floor and three standard floors, was examined in this analysis. The structural system of the building is a reinforced concrete moment frame with a reinforced concrete shear wall. The compressive strength of the concrete is 30 MPa, and S420 steel bars were used for both longitudinal and transverse reinforcement. The 3-D finite element model of the considered structure is shown in Figure 5.

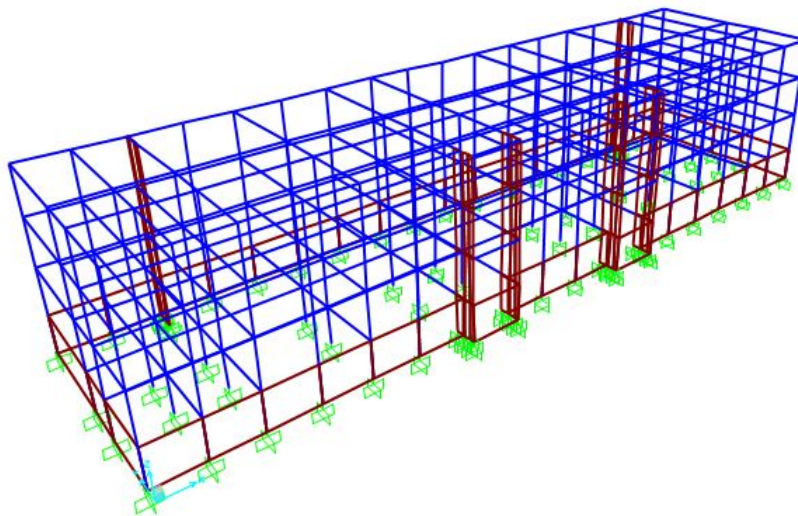


Figure 5. 3D numeric model of the existing school building

The fundamental period in the longitudinal direction (x-direction) of the structure was obtained as 0.687 seconds, while the fundamental vibration period for the short direction (y-direction) was calculated as 0.683 seconds. The modal mass participation ratios calculated for the x and y directions of the structure were 0.72 and 0.74, respectively. To implement the seismic vulnerability and risk analysis through a hybrid-based fragility curve, a pushover analysis is performed for an existing typical school building. The capacity curves are derived for each direction of the school building following a static non-linear analysis. The capacity curves obtained for both directions of the selected building are given in Figure 6.

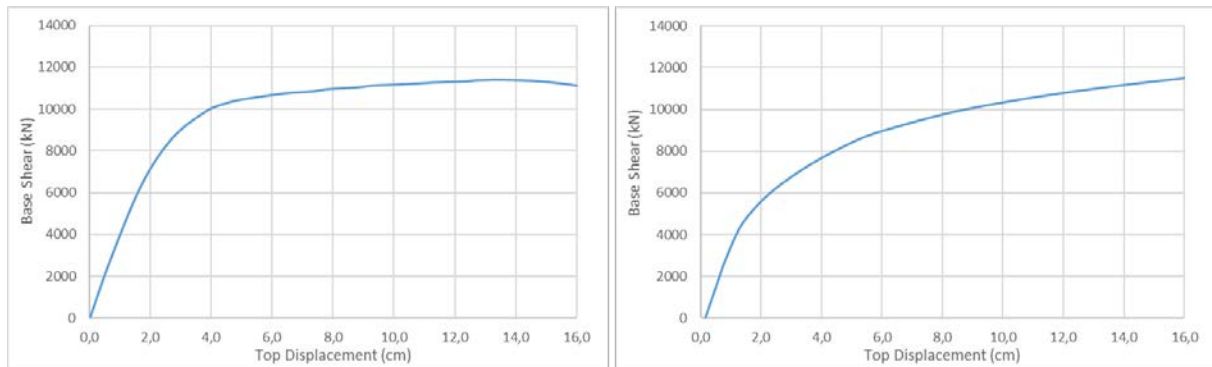


Figure 6. Capacity curves in both directions; X direction (left), Y direction (right)

2.5 Hybrid-Based Fragility Curves

As explained in the previous sections, the fragility curves are derived by utilizing the capacity curves along with the relevant empirical relations proposed by Lagomarsino and Giovinazzi (2006) [34], Vicente (2008) [35], and Lamego et al. (2017) [36]. The empirical relationships used to calculate the median values corresponding to different damage states considered in this study are presented in Table 1.

Table 1. Empirical relationships widely utilized in literature

Models	Median Spectral Displacement values			
	Slight ($S_{d,PS1}$)	Moderate ($S_{d,PS2}$)	Extensive ($S_{d,PS3}$)	Collapse ($S_{d,PS4}$)
Lagomarsino and Giovinazzi (2006) [34]	$0.7S_{dy}$	$1.5S_{dy}$	$0.5(S_{dy}+S_{du})$	S_{du}
Vicente (2008) [35]	$0.7S_{dy}$	$S_{dy}+(0.125S_{du})$	$(0.625S_{dy})+(0.5S_{du})$	$(0.125S_{dy})+(1.02S_{du})$
Lamego et al. (2017) [36]	$0.7S_{dy}$	S_{dy}	$S_{dy}+0.25(S_{du}-S_{dy})$	S_{du}

In this study, the equations based on ductility (μ), as defined within the framework of the Risk-UE Project and presented in Equation 3, were considered for the calculation of standard deviation (β_{DS_i}) values corresponding to each damage state [37].

$$\begin{pmatrix} \beta_1 = 0.25 + 0.07 \ln(\mu) \\ \beta_2 = 0.20 + 0.18 \ln(\mu) \\ \beta_3 = 0.10 + 0.40 \ln(\mu) \\ \beta_4 = 0.15 + 0.50 \ln(\mu) \end{pmatrix} \quad (3)$$

The fragility curves derived for both directions of the structure using three different empirical models are presented in Figures 7–9, respectively.

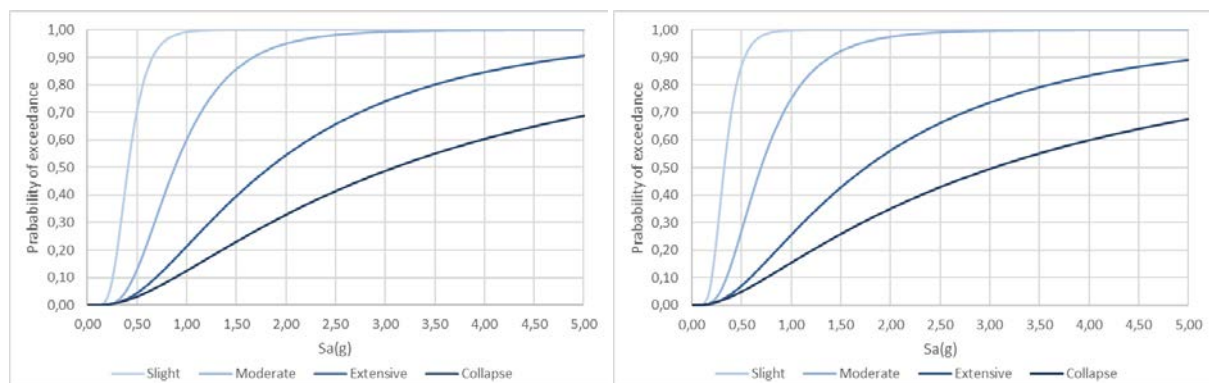


Figure 7. The fragility curves developed based on the model proposed by Lagomarsino and Giovinazzi (2006); the x-direction (left) and y-direction (right)

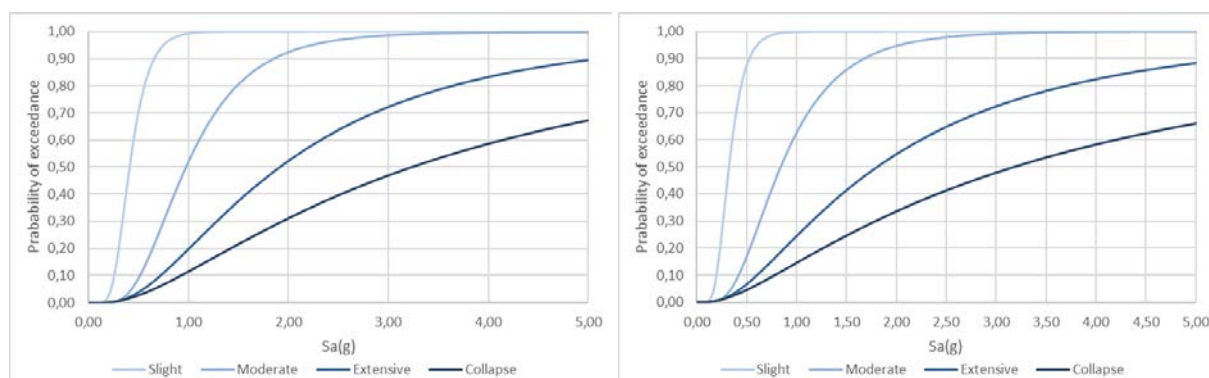


Figure 8. The fragility curves derived considering the model by the Vicente (2008); the x-direction (left) and y-direction (right)

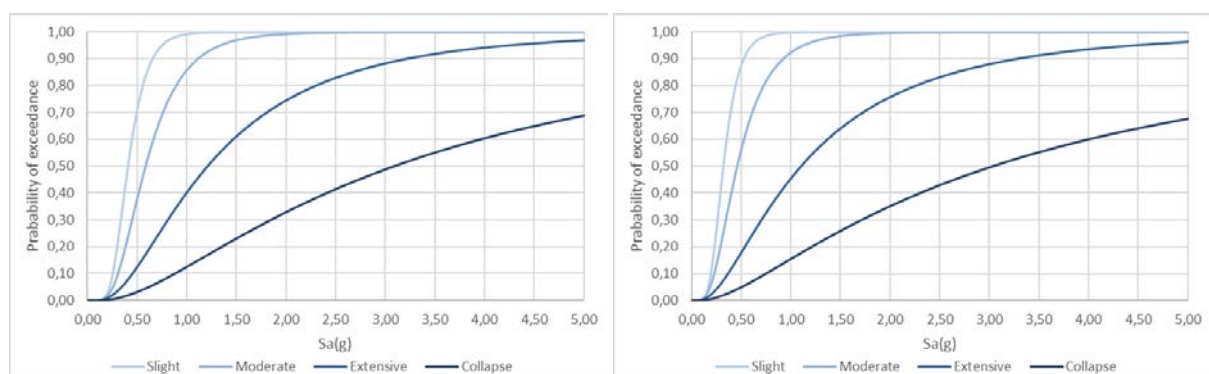


Figure 9. Fragility curves developed considering the model by Lamego et al. (2017), shown for the x-direction (left) and y-direction (right)

In Figures 7-9, fragility curves are developed as a function of spectral acceleration (S_a), based on different empirical relationships. As stated in previous sections, fragility curves represent the probability of exceeding a specific damage state for a given intensity measure (IM) level. These curves allow for seismic risk assessment by

considering the seismicity of the structure's location. However, to perform a comprehensive risk analysis, it is necessary to define the relationship between each considered damage state and the associated losses.

III. RESULTS AND DISCUSSIONS

The earthquake risk assessment methodology consists of three fundamental components: seismic hazard, vulnerability, and exposure. Numerous researchers have examined the impacts of earthquakes in terms of economic loss. Among these studies, the performance-based earthquake engineering (PBEE) methodology developed by the Pacific Earthquake Engineering Research Center (PEER), known as PEER-PBEE, has gained prominence due to its practical and simplified applications [38]. This methodology enables the estimation of both direct and indirect losses in a performance-based framework [39]. The PEER-PBEE approach is widely adopted in earthquake engineering [40, 41]. The main steps of this methodology include hazard analysis, structural analysis, damage assessment, and loss estimation.

In this study, the PEER-PBEE approach is employed to assess the seismic risk of school building. To carry out this assessment, it is essential to establish a relationship between a specific damage state and the associated losses (damage to loss functions). For this purpose, the Central Damage Ratio (CDR), also known as consequence models, is utilized. The consequence models commonly used in literature are presented in Table 2.

Table 2. Consequence models widely used in literature

Consequence Models	Central Damage Ratio				
	None	Slight	Moderate	Extensive	Collapse
Gurpinar et al. (1978) [42]	0,00	0,05	0,30	0,70	1,00
Askan and Yucemen (2010) [43]	0,00	0,05	0,30	0,85	0,85
DEE- KOERI (2003) [44]	0,05	0,20	0,50	0,80	1,00
Bal et al. (2008) [45]	0,00	0,16	0,33	1,00	1,00
FEMA (2010) [46]	0,02	0,10	0,50	1,00	1,00
Bramerini et al. (1995) [47]	0,01	0,10	0,35	0,75	1,00
Bommer et al. (2002) [48]	0,00	0,02	0,10	0,75	0,75
ATC-13 (1985) [12]	0,05	0,20	0,55	0,90	1,00
Tyagunov et al. (2006) [49]	0,05	0,10	0,40	0,80	1,00
Eleftheriadou (2011) [50]	0,00	0,05	0,15	0,65	1,00
Martins, & Silva (2021) [51]	0,00	0,05	0,20	0,60	1,00
Smyth et al. (2004) [52]	0,00	0,01	0,10	1,00	1,00

The fundamental difference between fragility and vulnerability curves is that, for a given IM value, fragility curves provide the probability of exceeding a specific damage state, whereas vulnerability curves indicate the probability of occurrence of the loss ratio. Therefore, fragility curves are typically derived as individual curves for each damage state, while vulnerability curves are developed as a single unified curve representing overall loss. The vulnerability curves have been calculated using the damage to loss functions provided in Table 2 and Equation 4. For a certain earthquake ground motion intensity value "j," the Loss Ratio, $(LR(S_{ae,j}))$, is determined by considering the probability of exceeding the "i" damage state, computed from the fragility curves $(P(DS_i|S_{ae,j}))$, and the CDR associated with the relevant "i" damage state (DS_i) as expressed in the consequence model.

$$LR(S_{ae,j}) = \sum_{DS} P(DS_i | S_{ae,j}) \times CDR(DS_i) \quad (4)$$

LR represents the ratio of the cost to repair the damage sustained by the structure after an earthquake to the total cost of the structure. Vulnerability curves are highly practical curves that provide the Loss Ratio (LR) value for a structure at a given Intensity Measure (IM) level. In this study, the twelve consequence models provided in Table 2 have been considered. Subsequently, the average of the vulnerability curves proposed for the risk analysis has been achieved. The vulnerability curves calculated for three different empirical models and for both directions of the structure are presented in Figures 10-12, respectively.

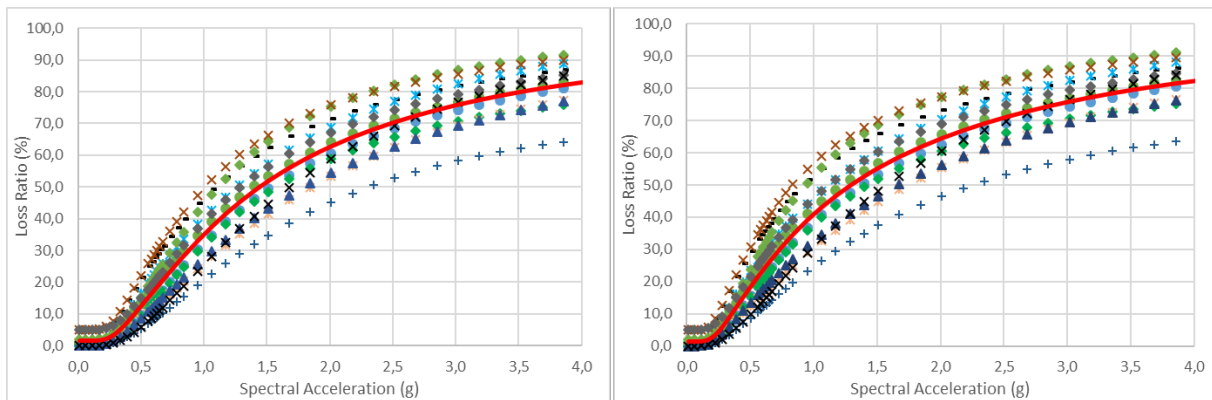


Figure 10. Vulnerability curves calculated for the Lagomarsino and Giovinazzi (2006) model; x-direction(left), y-direction(right)

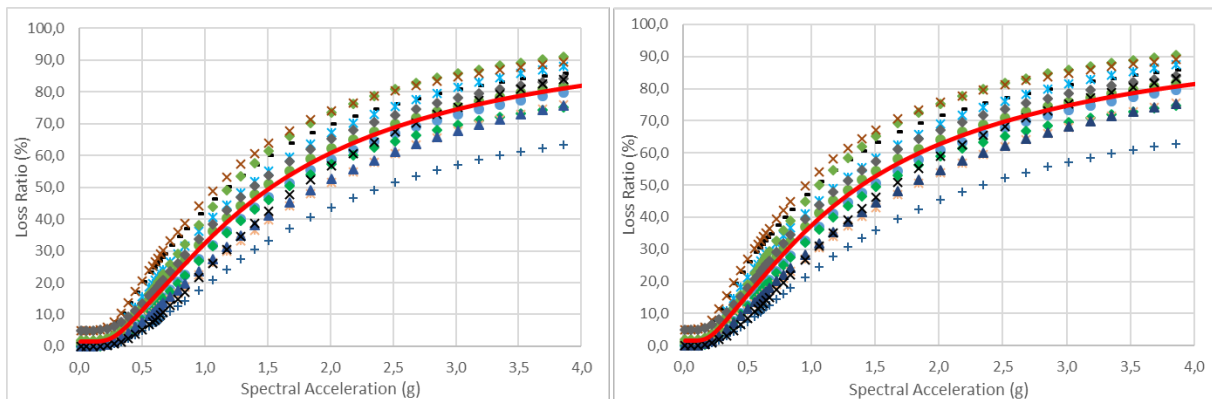


Figure 11. Vulnerability curves calculated for the Vicente (2008) model; x-direction (left), y-direction (right)

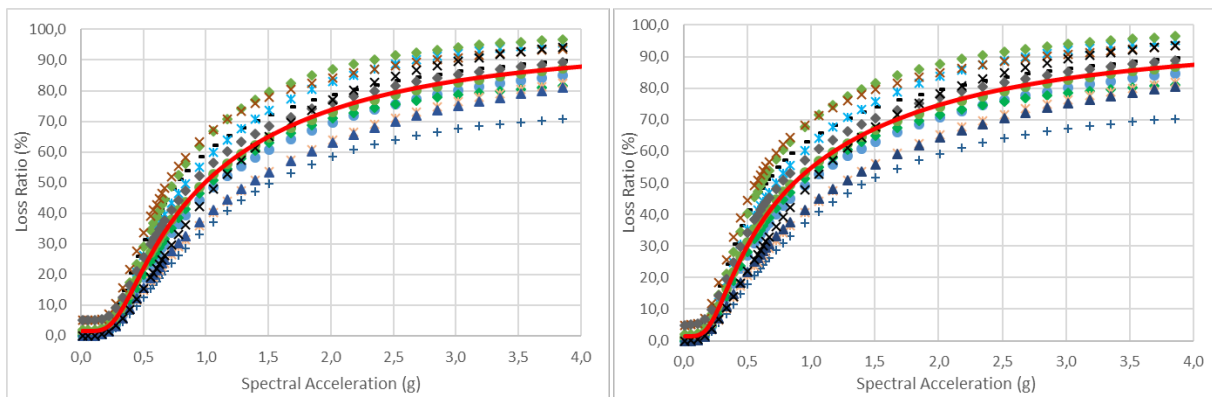


Figure 12. Vulnerability curves calculated for the Lamego et al. (2017) model; x-direction (left), y-direction (right)

In the average vulnerability curves calculated for different empirical functions, as presented in Figures 10-12, it is observed that the loss ratio values for the y-direction of the structure are higher for a given IM value. A seismic hazard analysis (SHA) was conducted for the Narince segment, as detailed in Section 2.2. In the event of fault rupture, the earthquake demand values for both directions of the structure considered in this study were calculated. Subsequently, the Expected Loss Ratio (ELR) for the school building was determined using the vulnerability curves and presented in Figure 13.

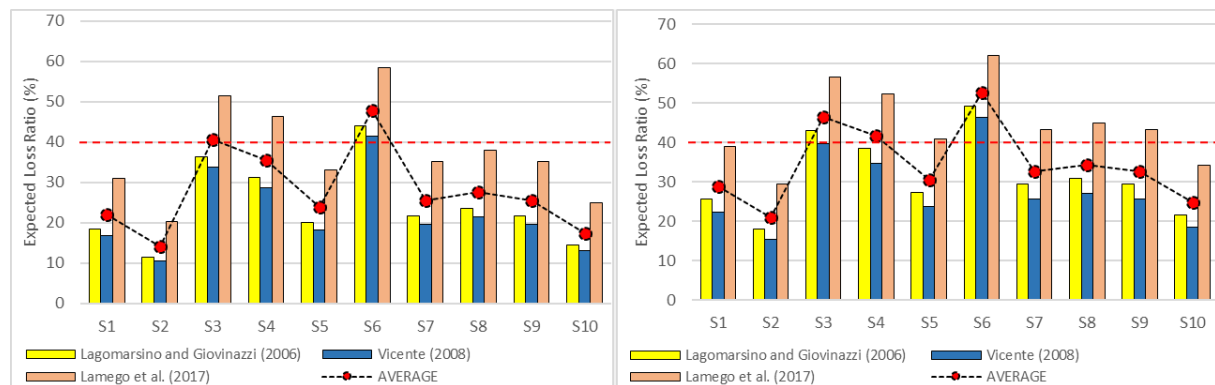


Figure 13. The ELR values calculated at various locations; a) in the x-direction(left), b) in the y-direction(right)

Figure 13 presents the ELR values calculated in both directions of the structure at all considered locations, using three different empirical models along with their average values. It is initially observed that the ELR values computed in the x- and y-directions are relatively close to each other. However, a slight increase in the ELR values is noticeable in the shorter direction of the structure (y-direction). This is primarily due to the fact that, as discussed in section 2.4, the lateral stiffness in both directions of the school building is designed to be extremely close. For instance, the average ELR value calculated at point S5 is 23.77% in the x-direction, whereas it reaches 30.65% in the y-direction. When the empirical models are evaluated individually, it is found that the lowest ELR values are obtained using the model proposed by Vicente (2008), while the highest values are derived from the model developed by Lamego et al. (2017).

Considering the average ELR values across different locations, the lowest value in the x-direction is calculated at point S2 as 14.12%, whereas the highest value is observed at point S6 with 47.93%. Similarly, in the y-direction, these values are 20.99% and 52.59% for points S2 and S6, respectively. The 40% ELR threshold is a subjective yet widely accepted criterion in relation to economic cost analysis [53]. When the ELR of a structure following an earthquake event exceeds this threshold, demolition and reconstruction of the building is generally considered more rational than retrofitting. Based on this criterion, it has been determined that the ELR values computed at locations S3 and S6 for the x-direction of the building exceed the specified threshold. A similar examination was conducted for the y-direction of the building; ELR values at locations S3, S4, and S6 were calculated to be higher than this limit. When the results are evaluated holistically, it is concluded that the school building considered in this study is likely to experience irreparable damage at points S3, S4, and S6. Conversely, at locations such as S1, S2, S5, and S10, the damage is expected to be moderate, and the structure may be rapidly repaired, allowing for

the continuation of educational services. If the methodology adopted in this study is applied to other types of school buildings, a more comprehensive seismic risk assessment can be conducted effectively.

IV. CONCLUSIONS

Seismic vulnerability and risk studies provide critical insights for the development of pre-earthquake action plans and post-earthquake decision-making processes. Recent earthquakes have shown that school buildings are particularly vulnerable to damage, often leading to significant disruptions in educational activities. The aim of this study is to conduct a seismic vulnerability and risk assessment of a typical low-rise reinforced concrete school building with shear wall systems located in the province of Adiyaman. To this end, hybrid fragility curves were derived for the representative school building based on various empirical models. Vulnerability curves were computed for twelve different consequence models, and the average vulnerability curve was utilized in the risk analysis. A scenario-based seismic hazard assessment was carried out by considering the potential rupture of the Narince segment, one of the active faults in the region. In addition, distributions of seismic ground motion intensity parameters such as PGA, $S_a(0.2s)$, and $S_a(1.0s)$ were obtained. Target spectra for each of the selected locations were also derived within the scope of the study. Based on average vulnerability curves developed through different empirical relationships and considering the seismicity of each location, the Expected Loss Ratio (ELR) values were calculated.

The results indicate that the ELR values for the examined school building vary significantly across different locations within the same province, ranging from 20.99% at location S2 to 52.59% at location S6. Moreover, the ELR values corresponding to the y-direction were consistently slightly higher than those of the x-direction across all locations. It was further observed that in some locations within the same province, specifically S3, S4, and S6, the structure is expected to experience irreparable loss levels. In contrast, at other locations such as S1, S2, S5, and S10, the loss levels remain within an economically repairable range that would allow the building to be returned to service within a short time. For the y-direction and location S9, the Expected Loss Ratio (ELR) values were calculated as 29.39%, 25.69%, and 43.29% based on the models proposed by Lagomarsino and Giovinazzi (2006), Vicente (2008), and Lamego et al. (2017), respectively. These results indicate notable variation in loss predictions depending on the selected empirical model.

In future studies, the classification of school buildings based on their material properties, structural system, construction year, and number of stories will enable more comprehensive risk assessment. In addition to the hybrid methodology, the derivation of analytically based fragility curves for this classification would provide valuable insights into their seismic vulnerability analysis. Moreover, the integration of similar risk assessment methodologies within a probabilistic seismic hazard analysis would support the formulation of region-specific preparedness and risk mitigation strategies. These advancements would contribute significantly to more resilient urban planning and disaster management practices.

ACKNOWLEDGMENT

The author sincerely thanks Senior Civil Engineers Seyhan Okuyan Akcan and Sinan Yazıcı for their valuable support and insightful comments.

REFERENCES

1. Chrysostomou CZ, Kyriakides N, Papanikolaou VK, Kappos AJ, Dimitrakopoulos EG, Giouvanidis AI (2015) Vulnerability assessment and feasibility analysis of seismic strengthening of school buildings. *Bulletin of Earthquake Engineering* 13: 3809-3840. <https://doi.org/10.1007/s10518-015-9791-5>
2. Saler E, Follador V, Carpanese P, Donà M, da Porto F (2024) Development of mechanics-based fragility curves for the Italian masonry school asset. *Earthquake Spectra* 40(3): 1905-1932. <https://doi.org/10.1177/87552930241245720>
3. Fotopoulou S, Karafagka S, Petridis C, Manakou M, Riga E, Pitilakis K (2023) Vulnerability assessment of school buildings: Generic Versus building-specific fragility curves. *Journal of Earthquake Engineering* 27(11): 2994-3023. <https://doi.org/10.1080/13632469.2022.2121791>
4. Yesilyurt A, Zulfikar AC, Tuzun C (2021) Seismic vulnerability assessment of precast RC industrial buildings in Turkey. *Soil Dynamics and Earthquake Engineering* 141: 106539. <https://doi.org/10.1016/j.soildyn.2020.106539>
5. Azizi-Bondarabadi H, Mendes N, Lourenço PB, Sadeghi NH (2016) Empirical seismic vulnerability analysis for masonry buildings based on school buildings survey in Iran. *Bulletin of Earthquake Engineering* 14: 3195-3229. <https://doi.org/10.1007/s10518-016-9944-1>
6. Giordano N, De Luca F, Sextos A, Ramirez CF, Fonseca FC, Wu J (2021) Empirical seismic fragility models for Nepalese school buildings. *Natural hazards* 105: 339-362. <https://doi.org/10.1007/s11069-020-04312-1>
7. Giordano N, De Luca F, Sextos A (2021) Analytical fragility curves for masonry school building portfolios in Nepal. *Bulletin of Earthquake Engineering* 19: 1121-1150. <https://doi.org/10.1007/s10518-020-00989-8>
8. Giusto S, Boem I, Alfano S, Gattesco N, Cattari S (2025) Derivation of seismic fragility curves through mechanical-analytical approaches: the case study of the URM school buildings in Friuli-Venezia Giulia region (Italy). *Bulletin of Earthquake Engineering* 23(6): 2611-2646. <https://doi.org/10.1007/s10518-025-02137-6>
9. Yesilyurt A, Zulfikar AC, Tuzun C (2021) Site classes effect on seismic vulnerability evaluation of RC precast industrial buildings. *Earthquakes and Structures* 21(6): 627-639. <https://doi.org/10.12989/eas.2021.21.6.627>
10. Di LM, Cattari S, Verderame G, Del Vecchio C, Ottonelli D et al (2023). Fragility curves of Italian school buildings: derivation from L'Aquila 2009 earthquake damage via observational and heuristic approaches. *Bulletin of Earthquake Engineering* 21(1): 397-432. <https://doi.org/10.1007/s10518-022-01535-4>
11. Sediqi Z, Harmandar E (2025) Improving the seismic resilience index of a school building. *Natural Hazards* 121(2): 2397-2417. <https://doi.org/10.1007/s11069-024-06990-7>
12. Applied Technology Council (ATC) (1985) Earthquake damage evaluation data for California, Report ATC 13, Applied Technology Council, Redwood City, CA.
13. ATC-21 (1988) Rapid Visual Screening of Buildings for Potential Seismic Hazards: A Handbook, Applied Technology Council, CA, FEMA 154.
14. Alcocer SM, Murià-Vila D, Fernández-Sola LR, Ordaz M, Arce JC (2020) Observed damage in public school buildings during the 2017 Mexico earthquakes. *Earthquake Spectra* 36(2): 110-129. <https://doi.org/10.1177/8755293020926183>
15. Domaneschi M, Noori AZ, Pietropinto MV, Cimellaro GP (2021) Seismic vulnerability assessment of existing school buildings. *Computers & Structures* 248:106522. <https://doi.org/10.1016/j.compstruc.2021.106522>
16. Gioiella L, Morici M, Dall'Asta A (2023) Empirical predictive model for seismic damage and economic losses of Italian school building heritage. *International Journal of Disaster Risk Reduction* 91:103631. <https://doi.org/10.1016/j.ijdrr.2023.103631>
17. O'Reilly GJ, Perrone D, Fox M, Monteiro R, Filiatrault A (2018) Seismic assessment and loss estimation of existing school buildings in Italy. *Engineering Structures* 168:142-162. <https://doi.org/10.1016/j.engstruct.2018.04.056>
18. Adhikari R, Gautam D (2019) Component level seismic fragility functions and damage probability matrices for Nepali school buildings. *Soil Dynamics and Earthquake Engineering* 120:316-319. <https://doi.org/10.1016/j.soildyn.2019.02.009>
19. Samadian D, Ghafory-Ashtiany M, Naderpour H, Eghbali M (2019) Seismic resilience evaluation based on vulnerability curves for existing and retrofitted typical RC school buildings. *Soil Dynamics and Earthquake Engineering* 127:105844. <https://doi.org/10.1016/j.soildyn.2019.105844>
20. Ruiz-García J, Olvera RN, Frías AD (2021) Seismic assessment of school buildings with short captive RC columns under subduction seismic sequences. *Structures* 34:2432-2444. <https://doi.org/10.1016/j.istruc.2021.09.019>

21. Sathurshan M, Thamboo J, Mallikarachchi C, Wijesundara K (2023) Seismic fragility of lightly reinforced concrete school building typologies with different masonry infill configurations. *Structures* 47:1710-1728. <https://doi.org/10.1016/j.istruc.2022.12.014>
22. Zain M, Dackermann U, Prasittisopin L (2024) Machine learning (ML) algorithms for seismic vulnerability assessment of school buildings in high-intensity seismic zones. *Structures* 70:107639. <https://doi.org/10.1016/j.istruc.2024.107639>
23. Mazılıgüney L (2020) Seismic Vulnerability Assessment of Reinforced Concrete School Buildings in Turkey. Dissertation, Middle East Technical University
24. Oyguc R, Guley E (2017) Performance assessment of two aseismically designed RC school buildings after the October 23, 2011, Van, Turkey Earthquake. *Journal of Performance of Constructed Facilities* 31(1): 04016076. [https://doi.org/10.1061/\(ASCE\)CF.1943-5509.0000938](https://doi.org/10.1061/(ASCE)CF.1943-5509.0000938)
25. Oyguc R (2016) Seismic performance of RC school buildings after 2011 Van earthquakes. *Bulletin of Earthquake Engineering* 14(3): 821-847. <https://doi.org/10.1007/s10518-015-9857-4>
26. Bal IE, Smyrou E (2016) Simulation of the earthquake-induced collapse of a school building in Turkey in 2011 Van Earthquake. *Bulletin of Earthquake Engineering* 14:3509-3528. <https://doi.org/10.1007/s10518-016-0001-x>
27. Altıok TY, Şevik M, Demir A (2024) Seismic performance of retrofitted and non-retrofitted RC school buildings after the February 6th, 2023, Kahramanmaraş earthquakes. *Bulletin of Earthquake Engineering* 1-36. <https://doi.org/10.1007/s10518-024-01941-w>
28. Republic of Türkiye, Governorship of Istanbul (2023) Press Release (2023-18) Directorate of Provincial Press and Public Relations. <http://www.istanbul.gov.tr/basin-aciklamasi-2023-18>
29. Hancilar U, Çaktı E, Erdik M, Franco GE, Deodatis G (2014) Earthquake vulnerability of school buildings: Probabilistic structural fragility analyses. *Soil Dynamics and Earthquake Engineering* 67:169-178. <https://doi.org/10.1016/j.soildyn.2014.09.005>
30. Mazılıgüney L, Yakut A, Kandaş K, Kalem İ (2013) Fragility analysis of reinforced concrete school buildings using alternative intensity measure-based ground motion sets. 2nd Turkish conference on earthquake engineering and seismology, Hatay, Turkey, September 25-27.
31. Emre Ö, Duman TY, Özalp S, Elmacı H, Olgun Ş, Şaroğlu F (2013) Active Fault Map of Turkey. General Directorate of Mineral Research and Exploration (MTA), Ankara.
32. Paganı M, Monelli D, Weatherill G, Danciu L, Crowley H, Silva V et al (2014) OpenQuake engine: An open hazard (and risk) software for the global earthquake model. *Seismological Research Letters* 85(3):692-702. <https://doi.org/10.1785/0220130087>
33. Boore DM, Stewart JP, Seyhan E, Atkinson GM (2014) NGA-West2 equations for predicting PGA, PGV, and 5% damped PSA for shallow crustal earthquakes. *Earthquake Spectra* 30(3):1057-1085. <https://doi.org/10.1193/070113EQS184M>
34. Lagomarsino S, Giovinazzi S (2006) Macroseismic and mechanical models for the vulnerability and damage assessment of current buildings. *Bulletin of Earthquake Engineering* 4:415-443. <https://doi.org/10.1007/s10518-006-9024-z>
35. Vicente R (2008) Estratégias e Metodologias para Intervenções ~ de Reabilitação ~ Urbana—Avaliação da Vulnerabilidade e do Risco Sísmico do Edificado da Baixa de Coimbra. Dissertation, University of Aveiro
36. Lamego P, Lourenço PB, Sousa ML, Marques R (2017) Seismic vulnerability and risk analysis of the old building stock at urban scale: application to a neighbourhood in Lisbon. *Bulletin of Earthquake Engineering* 15:2901-2937. <https://doi.org/10.1007/s10518-016-0072-8>
37. Mouroux P, Brun BL (2006) Presentation of RISK-UE project. *Bulletin of Earthquake Engineering* 4:323-339. <https://doi.org/10.1007/s10518-006-9020-3>
38. Günay S, Mosalam KM (2013) PEER performance-based earthquake engineering methodology, revisited. *Journal of Earthquake Engineering* 17(6):829-858. <https://doi.org/10.1080/13632469.2013.787377>
39. Yesilyurt A, Cetindemir O, Akcan SO, Zulfikar AC (2023) Fragility-based rapid earthquake loss assessment of precast RC buildings in the Marmara region. *Structural Engineering and Mechanics* 88(1):13-23. <https://doi.org/10.12989/sem.2023.88.1.013>
40. Cornell CA, Krawinkler H (2000) Progress and challenges in seismic performance assessment. PEER Center News, Spring 2000.
41. Krawinkler H, Deierlein GG (2014) Challenges towards achieving earthquake resilience through performance-based earthquake engineering. In: Fischinger M (ed) *Performance-based seismic engineering: Vision for an earthquake resilient society*, Geotechnical, geological and earthquake engineering, Vol 32. Dordrecht: Springer, pp. 3-23. https://doi.org/10.1007/978-94-017-8875-5_1
42. Gurbinar A, Abalı M, Yucemen MS, Yesilcay Y (1978) Feasibility of mandatory earthquake insurance in Turkey. Report No 78-05, Earthquake Engineering Research Center, Middle East Technical University.

43. Askan A, Yucemen MS (2010) Probabilistic methods for the estimation of potential seismic damage: Application to reinforced concrete buildings in Turkey. *Structural Safety* 32(4):262-271. <https://doi.org/10.1016/j.strusafe.2010.04.001>
44. DEE-KOERI (2003) Earthquake risk assessment for the Istanbul metropolitan area. Department of Earthquake Engineering, Kandilli Observatory and Earthquake Research Institute, Bogazici University Press, Istanbul, Turkey.
45. Bal İE, Crowley H, Pinho R, Gülay FG (2008) Detailed assessment of structural characteristics of Turkish RC building stock for loss assessment models. *Soil Dynamics and Earthquake Engineering* 28(10-11): 914-932. <https://doi.org/10.1016/j.soildyn.2007.10.005>
46. FEMA HMM (2010) Multi-hazard Loss Estimation Methodology/Earthquake Model/Technical Manual, Wasington DC, USA
47. Bramerini F, Di PG, Orsini A, Pugliese A, Romeo R, Sabetta F (1995) Rischio sismico del territorio italiano: Proposal of a methodology and preliminary results. National Seismic Survey Report, SSN/RT/ 95/01, Roma. <https://hdl.handle.net/11576/1892999>
48. Bommer J, Spence R, Erdik M, Tabuchi S, Aydinoglu N, Booth E, Del RD, Peterken O (2002) Development of an earthquake loss model for Turkish catastrophe insurance. *J. Seismol* 6:431-446. <https://doi.org/10.1023/A:1020095711419>
49. Tyagunov S, Grünthal G, Wahlström R, Stempniewski L, Zschau J, (2006) Seismic risk mapping for Germany. *Natural Hazards and Earth System Sciences* 6(4):573-586. <https://doi.org/10.5194/nhess-6-573-2006>
50. Eleftheriadou AK, Karabinis AI (2011) Development of damage probability matrices based on Greek earthquake damage data. *Earthquake Engineering and Engineering Vibration* 10(1):129-141. <https://doi.org/10.1007/s11803-011-0052-6>
51. Martins L, Silva V (2021) Development of a fragility and vulnerability model for global seismic risk analyses. *Bulletin of Earthquake Engineering* 19(15):6719-6745. <https://doi.org/10.1007/s10518-020-00885-1>
52. Smyth AW, Altay G, Deodatis G, Erdik M, Franco G, Güllkan P et al (2004) Probabilistic benefit-cost analysis for earthquake damage mitigation: Evaluating measures for apartment houses in Turkey. *Earthquake Spectra* 20(1):171-203. <https://doi.org/10.1193/1.1649937>
53. Yesilyurt A, Akcan SO, Cetindemir O, Zulfikar AC (2024) Probabilistic earthquake risk consideration of existing precast industrial buildings through loss curves. *Geomechanics and Engineering* 37(6):565-576. <https://doi.org/10.12989/gae.2024.37.6.565>